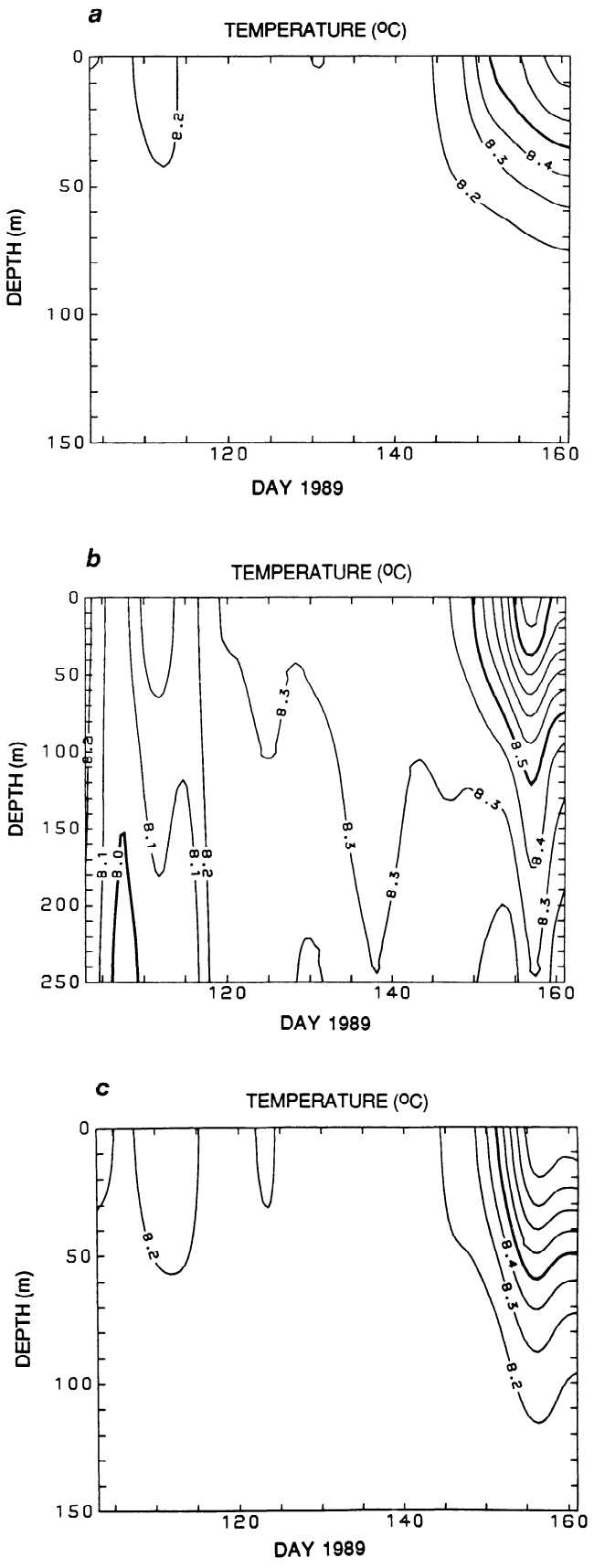

Figure 3. Time versus depth contours of water temperature: (a) one-dimensional Mellor-Yamada model simulation [*Emellor and Yamada*, 1982], (b) mooring data, and c) mooring data after subtracting temperature variability at 150 m.

reproduced by a one-dimensional model. Therefore we feel that a meaningful comparison of the calculated temperature with the data can only be made in terms of the relative rather than the absolute distributions. In order to separate "local" from "nonlocal" changes in water temperature (and following *Price et al.* [1986], we subtracted the temperature changes at 150 m from the temperature data. The temperature contours based on this calculation are shown in Figure 3c. Now the agreement between in situ temperature structure in the upper 150 m and the model simulation is fairly good. Because changes in salinity during the experiment were small, this temperature distribution is expected to be a good descriptor of the water density in the upper layer of the ocean.

In Figure 4 we have plotted mooring data, that is, fluorometrically determined concentration of Chl a (Figure 4a), and beam attenuation coefficient at 660 nm (c_{660}, Figure 4b). As a first approximation, c_{660} can be considered as a measure of the concentration of phytoplankton cells. The Chl a distribution predicted by the biophysical model with the E_o parametrization based on equation (5) is shown in Figure 5a. Relatively good agreement exists between model output and observations. Specifically, the slow increase of the Chl a concentration around day 110 is reproduced well by the model. This trend was perturbed near day 115 and again on day 140 apparently by high wind speeds and enhanced cooling of the surface water, which produced greater mixing (see time series of heat fluxes, *Stramska and Dickey*, 1993). Note also that our model results reproduce the bloom initiation before the seasonal thermocline is apparent in the temperature contours.

The model was also run using E_o parameterizations with equations (3) and (6) (equation (7) was not applied). The parameterization using Equation (3) gave similar results (not graphed here) to those associated with equation (5). In contrast, the model run with E_o described by equation (6) (Figure 5b, PAR averaged over the ML) did not reproduce the same phytoplankton pattern as parameterization by equations (3) and (5). The bloom occurred later, and a difference in the Chl a between the beginning and the end of the simulation period was greater than the observed one. This suggests that the vertical structure of the primary productivity in the water column (nearly exponential decrease with depth) is an important feature which should be included in phytoplankton models.

It is of interest to further consider the results of our calculations, focusing on the daily timescale. Biological variability on this timescale is thought to be in phase with the diel thermal cycle in the upper ocean [*Woods and Onken*, 1982; *Taylor and Stephens*, 1993]. This cycle is associated with the daytime absorption of solar radiation, which tends to warm and stabilize the near surface layer, and nighttime cooling, which together with wind mixing, acts to destabilize the water column [e.g., *Dickey and Simpson*, 1983; *Price et al.*, 1986; *Woods and Barkmann*, 1986].

Figure 6 shows vertical profiles of gains and losses of Chl a by vertical mixing (Figure 6a), losses representing respiration and grazing (Figure 6b), and gross primary production (Figure 6c), over a diel cycle. The changes of Chl a concentration in our model (Figure 6d) result from a local balance of these three components (see equation (10)). Figure 6 a shows that vertical mixing always acts to reduce biomass in the surface waters but can cause a gain at greater depths. Biomass losses by respiration and grazing (Figure 6b) are assumed to be proportional to the phytoplankton concentration. The